

What Can Really Be Learned from Dielectric Spectroscopy of Protein Solutions? A Case Study of Ribonuclease A

A. Oleinikova, P. Sasisanker, and H. Weingärtner*

Physical Chemistry 2, Ruhr-University, D-44780 Bochum, Germany

Received: January 28, 2004; In Final Form: April 1, 2004

We report on a dielectric relaxation study of aqueous solutions of ribonuclease A at 298.15 K as a function of protein concentration between 0.5 and 6 wt % in the MHz/GHz frequency range. The spectra can be decomposed into five modes of Debye type diffusive behavior. In agreement with the standard interpretation, we assign the two dominant modes at low and high frequency (β -relaxation and γ -relaxation, respectively) to protein tumbling and bulk water relaxation. We observe three further modes ($\delta 1$ – $\delta 3$) between β - and γ -relaxation, in contrast to a bimodal δ -dispersion frequently reported. We attribute the high frequency part ($\delta 3$) near 40 ps to hydration water reorientation, which, in the notion of other authors, corresponds to “loosely bound water”. We argue that the existence of “tightly bound” water, often deduced from the low frequency part in the nanosecond regime ($\delta 1$), is inconsistent with a highly mobile hydration layer observed by NMR techniques and molecular dynamics (MD) simulations. On the same grounds, we reject hydration water–bulk water exchange as a mechanism for δ -dispersion. In accordance with MD simulations, we assume that protein–water cross-correlations drive the nanosecond ($\delta 1$) process. We also discuss the role of intraprotein motions, which may contribute near 500 MHz ($\delta 2$). We discuss the meaning of the hydrodynamic radius and of the hydration numbers in light of the high mobility of hydration waters. We show that because of protein–protein interactions, the effective dipole moment of the protein decreases with increasing protein concentration.

1. Introduction

For understanding protein functions, a characterization of dynamical processes at the protein–solvent interface is of prime importance.¹ MHz/GHz dielectric spectroscopy probes processes between 10^{-6} and 10^{-12} s. In this regime, two strong dispersions reflect the reorientation of bulk water (“ γ -dispersion” near 20 GHz) and protein tumbling (“ β -dispersion” at 1–10 MHz). Much interest has focused on weak dispersions between the two (“ δ -dispersions”), which were attributed to processes at the protein–water interface, and served to derive detailed pictures of protein hydration.² Such assignments are plagued by diverse relaxation channels³ and have often relied on untested assumptions.

Meanwhile, X-ray and neutron scattering have provided details of hydration structures,⁴ and magnetic relaxation dispersion (MRD) experiments have unraveled many features of hydration dynamics.^{5–7} Molecular dynamics (MD) simulations have contributed to our knowledge of protein hydration⁸ and have given us insight into the mechanisms of dielectric relaxation.^{9–11} In addition, the power of modern network analyzers and computers now enables dielectric spectra to be recorded within minutes with an unprecedented frequency resolution. In conjunction with modern methods of statistical data analysis, this substantially improves the experimental basis. While some interpretations do not withstand the test of these developments, a proper embedding of dielectric relaxation into the framework of other experiments and simulations opens fascinating possibilities. This article aims to convey this major shift in perspective.

To broaden the experimental basis, we have conducted a case study of the single-domain pancreatic enzyme ribonuclease A (RNase A, 124 residues, 13.7 kDa), which has been used in many fundamental studies in biochemistry and biophysics.¹³ The X-ray crystal structure¹⁴ indicates three helices and two large antiparallel β -sheets, which form a V-shaped motif with one of the helices as a hinge. Local and global motions of the β -sheets control the access to the active center^{15,16} and play a key role for the protein function.¹⁷ Water molecules do not form an integral part of its structure, and there are only a few pockets of low water accessibility. The mobility of water at the protein surface and in these pockets has been studied by ²H and ¹⁷O MRD techniques.⁶ Results of two previous dielectric studies^{18,19} are, in parts, contradicting.

2. Methods

Samples. Solutions with mass fractions 0.005, $w_p \leq 0.06$ [concentrations $0.36 \leq C$ (mM) ≤ 4.38 mM] were prepared from bovine pancreatic RNase A (Sigma Chemical) and 5 mM Na₂HPO₄ buffer. They were adjusted to pH 5.5, where differential scanning calorimetry indicated high stability²⁰ and where RNase A is enzymatically highly active.²¹

Experiments. Dielectric reflection spectroscopy was used to monitor the real part $\epsilon'(\nu)$ (dielectric dispersion) and imaginary part $\epsilon''(\nu)$ (dielectric loss) of the complex permittivity $\epsilon^*(\nu)$. In the frequency range $300 \text{ kHz} \leq \nu = \omega/2\pi \leq 1.3 \text{ GHz}$, we employed the network analyzer 8712 ES (Agilent Technology) with a coaxial line terminating in a homemade sample cell of Kaatze’s design.²² At $200 \text{ MHz} \leq \nu \leq 20 \text{ GHz}$, we employed the network analyzer HP 8720 (Hewlett-Packard) and the probe HP 85070B. Spectra were recorded five times, in parts with freshly prepared solutions. All data refer to 298.15 K.

* To whom correspondence should be addressed. E-mail: hermann.weingaertner@ruhr-uni-bochum.de.

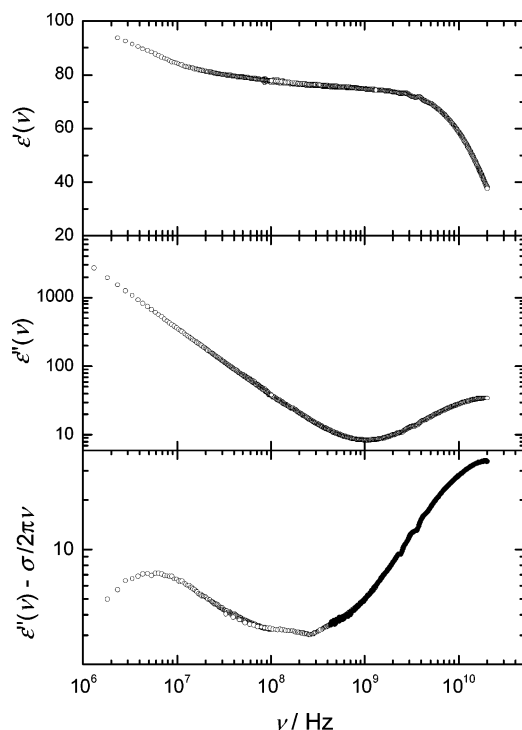


Figure 1. Real, imaginary, and conductance-corrected imaginary part of the dielectric spectrum of an aqueous solution of RNase A ($w_P = 0.06$, 5 mM phosphate buffer, pH 5.5, 298.15 K). Data points measured by two different apparatus are given by different symbols.

The complex dielectric permittivity of an electrically conducting system is given by^{2,23}

$$\epsilon^*(\omega) = \epsilon'(\omega) - i\epsilon''(\omega) = \epsilon_\infty + \Delta\epsilon'(\omega) - i\Delta\epsilon''(\omega) + \frac{\sigma}{i\epsilon_0\omega} \quad (i^2 = -1) \quad (1)$$

Figure 1 shows the real part, $\epsilon'(\nu)$, and the imaginary part, $\epsilon''(\nu)$, of the permittivity of a concentrated solution. We are interested in the relaxational terms $\Delta\epsilon'(\omega)$ and $\Delta\epsilon''(\omega)$. Electronic and vibrational processes are often accounted for by a limiting value $\epsilon_\infty \cong n^2$ of the real part, where n is the optical refractive index.²³ For pure water, $n^2 \cong 1.78$. Because of the processes in the terahertz regime, dielectric relaxation data for pure water below 100 GHz extrapolate, however, to $\epsilon_\infty = 5.2$.²⁴ The latter value was adopted in further data processing. The results proved to be insensitive to moderate variations of ϵ_∞ , by say ± 1 .

The static (d.c.) conductivity, σ , gives rise to a low frequency response of $\epsilon''(\nu)$, which diverges as $\sigma/i\epsilon_0\omega$, where ϵ_0 is the permittivity of the vacuum. The conductivity of the buffer solution at pH 5.5 was $\sigma \cong 0.104 \Omega^{-1} \text{ cm}^{-1}$; those of the protein solutions were up to three times as large. Figure 1 shows the conductance-corrected imaginary part, $\Delta\epsilon''(\nu)$. The accuracy of the correction was ensured by examining the Kramers–Kronig relation,²³ which relates $\Delta\epsilon'(\nu)$ to $\Delta\epsilon''(\nu)$. Even small errors lead to substantial violations of this relation. On the basis of such an analysis, we rejected all data points recorded below 2 MHz.

Spectral Analysis. Figure 1 suggests a superposition of distinct dispersions, each represented by a spectral term $J_k(\omega)$

$$\epsilon^*(\omega) = \epsilon_\infty + \sum_{k=1}^k J_k(\omega) \quad (2)$$

Denoting the relaxation time by τ_k and the amplitude by S_k ,

Debye's model of the small step rotational diffusion of a sphere provides an expression for $J_k(\omega)$ of the form²³

$$J_k(\omega) = \frac{S_k}{1 + i\omega\tau_k} \quad (3)$$

For ellipsoids of moderate anisotropy, the form of eq 3 does not markedly change.²⁵ Distributions of relaxation times can be accounted for by the exponents α and β in the more general expression²³

$$J_k(\omega) = \frac{S_k}{[1 + (i\omega\tau_k)^{1-\alpha}]^\beta} \quad (4)$$

Eq 4 comprises well-known limiting cases:^{2,23} the Debye equation ($\alpha = 0, \beta = 1$), the symmetrical Cole–Cole distribution of relaxation times ($0 < 1 - \alpha < 1, \beta = 1$), and the asymmetrical Cole–Davidson distribution ($\alpha = 0, 0 < \beta < 1$). In the literature, up to six terms $J_k(\omega)$ were tried. Significant parametrizations are, however, subject to physical bounds and should provide robust and unique solutions with low parameter correlations. Many controversies in the literature may have resulted from an inadequate parametrization by inappropriate fitting procedures and/or low frequency resolution.

We performed simultaneous fits of $\Delta\epsilon'(\omega)$ and $\Delta\epsilon''(\omega)$. Despite the low frequency cutoff imposed on the data and the experimental high frequency cutoff at 20 GHz, the β - and γ -dispersions were sampled over sufficient frequency ranges to ensure an accurate parametrization. Both modes were perfectly describable by Debye behavior. The challenge was to evaluate the weak δ -dispersions. Because the fit parameters of the β - and γ -dispersions proved to be independent from the representation of the remaining modes, we subtracted these two modes from the spectrum. The difference spectrum, $\epsilon_\delta^*(\nu)$, reflects the δ -dispersion only. Because this step in data processing may be particularly sensitive to systematic errors, we extensively modeled error propagation by varying the parameters of the β - and γ -modes within reasonable ranges. Within the limits quoted in Table 1, the basic spectral structure of the difference spectra $\epsilon_\delta^*(\nu)$ remained unaffected. However, the difference spectra also absorbed and magnified artifacts in the primary data such as spikes and weak apparatus specific oscillations. These artifacts were removed by spline digital filtering of the difference spectra, using the NURBS algorithm.²⁶

An example for the filtered imaginary part, $\epsilon_\delta''(\nu)$, is shown in Figure 2. This figure suggests the presence of three dispersion regions, numbered from low to high frequency by $\delta 1$ – $\delta 3$. For compositions $w_P \geq 0.015$, this three term structure behaved reproducibly in repeated experiments and robustly with regard to details of data processing. It was also present in the unfiltered spectra. In the literature, δ -dispersion was often claimed to be bimodal,^{2,27} $\Delta\epsilon''(\nu)$ presumably reflecting a lower frequency resolution in earlier work. At compositions below $w_P = 0.015$, only fits with two δ -terms provided unique solutions. In these cases, only the fit parameters of the β - and γ -modes are physically significant.

In data fitting, only Debye terms gave robust results for the three δ -dispersions. The $\delta 1$ mode near 100 MHz could be fitted with high accuracy. At high concentrations, it reveals itself by a distinct peak. The amplitude of $\delta 3$ near 5 GHz is comparable with that of $\delta 1$, but because of the wing of the intense γ -dispersion, at the peak maximum, the intensity of $\delta 3$ amounts to less than 15% of the intensity of $\epsilon''(\nu)$. At sufficiently high protein concentrations, no adequate representation of the spectra

TABLE 1: Parametrization of Dielectric Spectra of Aqueous Solutions of RNase A at 298.15 K (5 mM Phosphate Buffer, pH 5.5)

| w_p | C (mM) | τ_β (ns) | $\tau_{\delta 1}$ (ns) | $\tau_{\delta 2}$ (ps) | $\tau_{\delta 3}$ (ps) | τ_γ (ps) | S_β | $S_{\delta 1}$ | $S_{\delta 2}$ | $S_{\delta 3}$ | S_γ | ϵ_s | a (nm) |
|------------------------------|----------|-------------------|------------------------|------------------------|------------------------|--------------------|-----------|----------------|----------------|----------------|------------|--------------|----------|
| 0.005 ^a | 0.36 | 20.5 | 2.8 | | | 8.35 | 2.13 | 0.81 | | | 73.0 | 81.1 | 1.97 |
| 0.01 ^a | 0.72 | 22.0 | 2.8 | | | 8.35 | 4.20 | 1.31 | | | 73.0 | 83.4 | 2.01 |
| 0.015 ^b | 1.08 | 26.4 | 3.00 | 558 | 38.3 | 8.49 | 7.66 | 1.73 | 0.72 | 0.97 | 71.1 | 87.5 | 2.11 |
| 0.02 | 1.46 | 26.9 | 3.00 | 547 | 37.0 | 8.28 | 10.7 | 1.60 | 1.00 | 1.30 | 70.5 | 90.3 | 2.15 |
| 0.03 | 2.19 | 26.8 | 2.98 | 426 | 36.6 | 8.60 | 11.3 | 2.35 | 2.08 | 2.30 | 69.1 | 92.5 | 2.15 |
| 0.04 ^c | 3.06 | 26.7 | 2.95 | 500 | 36.6 | 8.30 | 14.0 | 2.77 | 2.54 | 3.00 | 66.8 | 95.0 | 2.14 |
| 0.06 | 4.38 | 27.3 | 2.77 | 510 | 34.8 | 8.13 | 14.7 | 3.53 | 2.06 | 3.22 | 66.3 | 95.4 | 2.16 |
| uncertainty (%) ^d | | 2–5 | 10 | 10–20 | 10 | 2 | 2–10 | 2–5 | 10–20 | 5–20 | 1 | <1 | 2–5 |

^a Unique solutions were only obtained by four term fits. ^b A four term fit of this spectrum was reported previously.^{25b} ^c A second solution with the same standard deviation was rejected, because $\tau_{\delta 3} = 48.6$ ps did not smoothly join with data obtained at the other concentrations. ^d The quoted intervals refer to estimates from high to low concentrations.

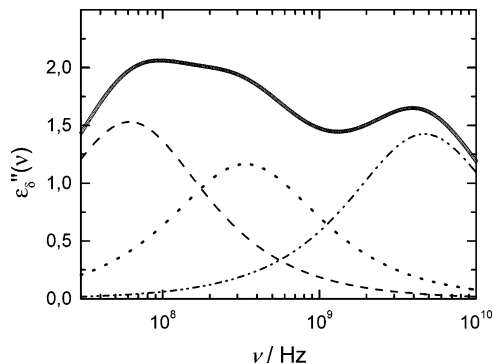


Figure 2. Residual part of the spectrum in Figure 1 (imaginary part only) after subtracting the dominant β - and γ -dispersions, followed by digital filtering and decomposition into three Debye modes. For details, see the text.

could, however, be obtained without accounting for a mode near 5 GHz. Similar dispersions were also reported for other proteins such as myoglobin.² The parameters of the weak mode near 500 MHz ($\delta 2$) were sensitive to details of data processing. Although fitted to a distinct mode, this dispersion may represent a broad background. No adequate representation of the spectra could be obtained without accounting for a contribution near 500 MHz.

The final parametrization is summarized in Table 1. Uncertainties of the fit parameters in the last line of this table refer to estimates at the lowest and highest concentrations, as assessed from their reproducibility in repeated experiments and with different samples. For filtered spectra, standard deviations of the fits are meaningless.

3. Spectral Assignment

Component Analysis of Dielectric Spectra. In the rigorous dielectric relaxation theory of mixtures,^{11,12,28} the quantity of interest is the time correlation function of the total dipole moment $\mathbf{M}(t)$ of the system, $\Phi(t) = \langle \mathbf{M}(t) \cdot \mathbf{M}(0) \rangle$, which upon Fourier–Laplace transformation yields $\epsilon^*(\omega)$. Bold quantities refer to vectors. In a n -component system, $\mathbf{M}(t)$ is a sum of component contributions $\mathbf{M}_i(t)$ ^{11,12}

$$\Phi(t) = \left\langle \sum_{i=1}^n \mathbf{M}_i(t) \cdot \sum_{j=1}^n \mathbf{M}_j(0) \right\rangle = \sum_{i=1}^n \sum_{j=1}^n \Phi_{ij}(t) \quad (5)$$

where in standard hydration models for simple solutes, hydration water and bulk water are treated as distinct components.^{29,30} A similar classification is usually adopted for protein solutions.² Sometimes, it may be necessary to account for more than three components, for example, when treating effects caused by metal ions or protons.

Considering a ternary system comprising the protein (P), hydration water (H), and bulk water (B) and noting that $\Phi_{ij}(t) = \Phi_{ji}(t)$, eq 5 gives rise to six component correlation functions.^{11,12} The functions $\Phi_{PP}(t)$, $\Phi_{HH}(t)$, and $\Phi_{BB}(t)$ are self-correlation functions ($i = j$), which reflect dipole moment fluctuations due to component reorientation. If each function is monoexponential, the spectrum consists of three Debye modes, corresponding to popular hydration models.^{2,29} According to common wisdom, the dominating β - and γ -processes reflect protein tumbling and bulk water reorientation, respectively, while hydration water reorientation should reveal itself in the δ -regime.

There are several options for rationalizing spectra exhibiting more than three modes. For example, self-terms may be multimodal. A multimodal structure of $\Phi_{HH}(t)$ may be founded in the heterogeneity of the protein surface and may give rise to different states of hydration water. An example is an often claimed bimodality of δ -dispersion, due to “tightly bound” and “loosely bound” hydration water.^{2c} A bimodal structure of the self-term $\Phi_{PP}(t)$ may result from intraprotein motions superimposed on protein tumbling.^{9–11} A fundamentally different scenario considers, however, the cross-terms $\Phi_{PH}(t)$, $\Phi_{PB}(t)$, or $\Phi_{HB}(t)$ to drive relaxation. Such terms are usually neglected in data analysis, but their relevance is found in recent MD simulations^{11,12} and their comparison with experiment.³¹ For simple systems, the presence of cross-terms is now well-established by experiment,^{28,32} theory,^{28,33} and simulations.^{28,30,34}

In view of this diversity of relaxation channels, a proper embedding of data interpretation into the framework of results from other experiments and from simulations is mandatory. Some scenarios will now be discussed in detail. To facilitate this discussion, Table 2 compares our assignment with two widely adopted interpretations.

Protein Tumbling. β -Dispersion is assigned to protein tumbling. For RNase A (600 μ M, pH 6.4, 10 mM NaCl, 298 K), the reorientation time deduced from ¹⁵N relaxation is 6.5 ns.¹⁶ Reorientation times determined by NMR depend on rank two spherical harmonics, while dielectric relaxation probes first rank spherical harmonics. For diffusive single-particle reorientation, the reorientation times differ by a factor of 3.²³ Thus, $\tau_\beta \cong 3\tau_{\text{NMR}} \cong 19.5$ ns, in perfect agreement with the low concentration values in Table 1.

In protein solutions, the static dielectric constant, ϵ_s , increases over the value of pure water (“dielectric increment”). Simple solutes show a decrease.^{4,29} ϵ_s is defined as the zero-frequency limit of $\epsilon'(\omega)$, given by the sum of the amplitudes S_k (plus ϵ_∞). According to Table 1, the decrease of S_γ is overcompensated by an increase of the other terms, S_β yielding the major contribution. It has recently been conjectured^{27b,c} that an increment implies unphysically high dipole moments of proteins.

TABLE 2: Assignment of the Dielectric Spectrum of RNase A as Compared with Interpretations Given in the Literature^a

| mode | β | $\delta 1$ | $\delta 2$ | $\delta 3$ | γ |
|----------------------------|--------------------------|----------------------------|------------------------------------|---------------------|----------------|
| time scale | 25 ns | 2 ns | 500 ps | 35 ps | 8.3 ps |
| assignment | $\Phi_{pp}(t)$ | $\Phi_{HH}(t)$ | $\Phi_{pp}(t)$ (?) | $\Phi_{HH}(t)$ | $\Phi_{BB}(t)$ |
| interpretation | protein tumbling | protein–water interactions | polar side chains (?) ^b | hydration water | bulk water |
| Pethig ³ | protein tumbling | tightly bound water | | loosely bound water | bulk water |
| Nandi et al. ³² | protein tumbling doubted | water exchange | | water exchange | bulk water |

^a For details, see the text. ^b Protein–bulk water interactions [term $\Phi_{PB}(t)$ in eq 5] may also form a relaxation mechanism in this regime.^{13,14}

Protein structures yield dipole moments of hundreds of Debye (1 D = 3.30×10^{-30} C m).³⁵ Using expressions quoted later, it is a simple exercise to prove the dominating effect of the β -mode upon the increment.

Intraprotein Motions. It has sometimes been speculated that δ -dispersion at the nanosecond scale ($\delta 1$) is driven by internal motions of the protein.² NMR studies locate changes in the secondary structure (“conformational exchange”) below the MHz/GHz frequency range, while motions in disordered regions, the bending of helices, and the predicted¹⁵ breathing of β -sheets may fall into the MHz/GHz range.³⁶ Cole and Loria¹⁶ have concluded from ¹⁵N relaxation data that RNase A is comparatively rigid at the time scale of protein tumbling.

Another option is the side chain dynamics of solvent-exposed, polar, and charged groups. NMR studies of side chain dynamics indicate a wide range of time scales from picoseconds to nanoseconds.^{36,37} While the presence of such processes in the MHz/GHz region is undoubted, it is difficult to assess the magnitude of the resulting dipole moment fluctuations. There are, however, hints from MD simulations that such processes indeed play a role in dielectric relaxation.^{10–12} In particular, Simonson and Perahia^{10b} observed dipolar fluctuations of polar groups of cytochrome *c* to contribute to the dielectric spectrum at 100–800 ps. Simulations of a zinc finger peptide by Steinhäuser and co-workers¹² revealed a bimodal correlation function $\Phi_{pp}(t)$, with a fast component (162 ps) driven by the solvent-exposed polar groups. These results imply dielectric processes at the time scale of some 100 ps, possibly driving the $\delta 2$ process near 500 MHz. The results are inconsistent with an assignment of a nanosecond mode ($\delta 1$) to such processes.

Hydration Water Reorientation. Interpretations of δ -relaxation have usually focused on processes involving hydration water. Following the work of Grant, as summarized in a much-cited review by Pethig,^{2c} many workers have presumed a bimodal nature of δ -dispersion, attributed to two sorts of hydration water, namely, “loosely bound water” with a picosecond relaxation time (40 ps for myoglobin, corresponding to $\delta 3$) and “tightly bound water” with a nanosecond relaxation time (10 ns, corresponding to $\delta 1$).

We know now that this picture must be wrong. MRD experiments^{5–7} and MD simulations⁸ indicate fast reorientation of almost all water molecules in the hydration layer of the protein and fail to detect the nanosecond component ($\delta 1$) of the postulated bimodal behavior. ²H and ¹⁷O MRD experiments for a large number of globular proteins show that virtually all water molecules in the hydration layer are only retarded by a factor of 2–3 as compared to bulk water, as also found for simpler solutes.^{4–6,38} The crystal structure of RNase A¹⁴ identifies six pockets of lower water accessibility, corresponding to about 1% of the total number of hydration waters. Three strongly retarded water molecules in such pockets were observed in MRD experiments.⁶ At the concentrations used here, about 100 waters per protein are required to generate a detectable dielectric signal. Thus, the modes $\delta 1$ and $\delta 2$ must be of different origins.

On the basis of $\tau_\gamma \cong 8.5$ ps, we expect from MRD data a relaxation time of 15–25 ps. Mode $\delta 3$ with $\tau_{\delta 3} \cong 35$ ps comes close to this estimate and possesses the expected amplitude (see later). We have no doubt that this mode signals hydration water. At a quantitative level, the retardation factor $\tau_{\delta 3}/\tau_\gamma \cong 4.5$ is, however, distinctly larger than the factor of 2–3 observed by NMR. In seeking for a consistent picture, this discrepancy is disturbing. However, rigorous dielectric relaxation theory provides a subtle explanation. The best available data for pure water yield $\tau_{\text{diel}} \cong 4.5\tau_{\text{NMR}}$ rather than $\tau_{\text{diel}} \cong 3\tau_{\text{NMR}}$ and even larger deviations are observed for some other fluids.³² This discrepancy reflects collective contributions to dielectric relaxation. As first shown by Madden and Kivelson³³ and recently confirmed experimentally³² and by simulations,³⁴ a better approximation is

$$\tau_{\text{diel}} = 3g_K\tau_{\text{NMR}} \quad (6)$$

where g_K is the Kirkwood correlation factor,^{23,39} which describes contributions of orientational correlations among the dipoles to the static dielectric constant. For preferred antiparallel orientations, $g_K < 1$, and for parallel correlations, $g_K > 1$. The value $g_K > 1$ for water²³ indicates parallel correlations founded in the water structure. Introducing Kirkwood factors $g_{K,H}$ and $g_{K,B}$ for hydration water and bulk water, respectively, we find at this level of approximation for the retardation of hydration water observed by dielectric relaxation

$$\xi_{\text{diel}} = \frac{\tau_{\delta 3}}{\tau_\gamma} = \frac{g_{K,H}}{g_{K,B}} \xi_{\text{NMR}} \quad (7)$$

where ξ_{NMR} is the retardation factor observed by NMR. MD simulations⁴⁰ reveal enhanced parallel orientations of water in the hydration layer as compared to the bulk, so that $g_{K,H} > g_{K,B}$. According to eq 7, this slows down the dielectric process, as is actually observed.

Hydration Water–Bulk Water Exchange. Nandi and Bagchi have recently suggested that δ -dispersion may be found in the cross-terms ($i \neq j$) of eq 5.²⁷ In particular, they developed^{27a} and appraised^{27c} a theory in which δ -dispersion was attributed to the exchange of water molecules from the protein surface to the bulk. In terms of eq 5, such exchange contributions are covered by the term $\Phi_{HB}(t)$. For simple fluids, contributions of such chemical rate processes to dielectric relaxation have been treated for a variety of situations,²³ including hydration water exchange.⁴¹ Nandi and Bagchi’s theory rationalizes a “universal” bimodal relaxation process with a picosecond and a nanosecond mode. However, the prediction of a nanosecond mode is merely a consequence of the erroneous input, that hydration water dynamics is rigidly coupled to protein reorientation.

Among others, Nandi and Bagchi justify their model by intermolecular nuclear Overhauser (NOE) experiments,⁴² which were interpreted in terms of nanosecond residence times of water at the protein surface. We know now that this picture is wrong. MRD^{5–7} measurements and MD simulations^{8b,43} indicate trans-

lational motions of almost all water molecules to occur at the same time scale as molecular reorientation, i.e., 10–50 ps. The rationale is that the formation and breaking of hydrogen bonds is rate-limiting for rotation and translation. In contrast to common belief, intermolecular NOE data, on the other hand, do not provide information on these exchange processes. In refs 7 and 44, it has been convincingly demonstrated that there are fundamental limitations to intermolecular NOE measurements, which imply that the existing data are dominated by long-range protein–bulk water correlations of no direct relevance to the hydration issue. A few molecules in crevices and clefts may give rise to a long-time tail of the residence time distribution and may indeed affect the intermolecular NOE. As noted, the number of retarded water molecules buried in pockets of RNase A is marginal.⁶

Protein–Water Cross-Interactions. The mechanisms discussed hitherto give little evidence for a process driving a nanosecond mode. Any reliable assignment of the $\delta 1$ mode has to explain why a nanosecond process is present, even though only fast hydration dynamics is present. As emphasized by us,³¹ a straightforward rationale is found in MD simulations by Steinhauser' groups.^{11,12} These simulations identify protein–water cross-correlations as a source for slow δ -relaxation. In eq 5, this attributes relaxation to the cross-terms $\Phi_{PH}(t)$ and $\Phi_{PB}(t)$, in contrast to Nandi and Bagchi's model, which considers the cross-term $\Phi_{HB}(t)$ to drive relaxation. In heuristic models and in most MD simulations, these cross-terms are implicitly or explicitly neglected. For simple systems, their importance is known from the theory of the static dielectric constant, where they are accounted for by the Kirkwood correlation factor.^{23,39} There is now ample evidence that such cross-correlations affect time-dependent dielectric properties as well.^{28,30,32–34} These collective modes may be slow, and the interacting particles may move comparatively rapidly.³² Similar phenomena are expected in more complex systems.

In fact, a comparative analysis of MD and experimental data for ubiquitin³¹ showed that the simulated mode corresponding to $\Phi_{PH}(t)$ satisfied all experimental features and reflected also the basic features of mode $\delta 1$ in the spectrum of RNase A. The process is located close to the β -mode, and the amplitudes are 20–50% of that of β -relaxation. The process is collective and therefore not observable in MRD experiments. Note that in simulations even the term $\Phi_{PB}(t)$ for protein–bulk water coupling has shown up near 100–200 ps.^{11,12} As an alternative to the explanation in terms of side chain motions, there therefore is some room left for attributing mode $\delta 2$ to long-range protein–bulk water interactions (but not for the faster $\delta 3$ mode).

Counterion Diffusion at the Protein Surface. An additional mechanism may result from the displacement of counterions at the surface of charged proteins.² In the framework of eq 5, such a mechanism would imply counterions to be treated as a further distinct component. The isoelectric point of RNase A is $pI = 9.3$.⁴⁵ At pH 5.5, the net charge of RNase A is about $z = +8$.⁴⁶ For some charged surfactants, contributions of counterion diffusion in the MHz/GHz regime seem to be well-established;⁴⁷ for proteins, they have often been assigned to the kHz regime.² There are reliable theoretical approaches, for example, a model by Grosse,⁴⁸ which suggest that such modes cannot play a role in the system treated here. Even for highly charged micelles, the respective modes are rather weak.⁴⁷

Final Assignment. In agreement with the generally accepted interpretation, we assign the dominant processes (β and γ) to protein tumbling and bulk water relaxation. We certify that protein tumbling causes the dielectric increment. We confirm

the multimodal structure of the δ -dispersion but observe three contributions rather than an often-quoted bimodal structure. We attribute the high frequency part, $\delta 3$, to hydration water reorientation, which corresponds to the loosely bound water found by other workers. The existence of tightly bound water, often deduced from the low frequency part, $\delta 1$, is inconsistent with observations from other experiments and simulations. On the same grounds, we reject hydration water–bulk water exchange as mechanisms for δ -dispersion. In accordance with MD simulations, we assume protein–water cross-correlations to form the source of the nanosecond process, $\delta 1$. Its collective nature explains the absence of such a process in MRD experiments. We speculate that fluctuations of polar side chains may drive a mode at the subnanosecond time scale ($\delta 2$).

4. Microscopic Parameters Extracted from Dielectric Relaxation Spectra

Hydrodynamic Radii of Proteins. The reorientation of a globular protein is a typical example of a process controlled by the hydrodynamic friction of the solvent.² For a spherical protein, the (first rank) tumbling time of a sphere of hydrodynamic radius a and hydrodynamic volume V in a medium of viscosity η (here, $\eta = 0.90 \times 10^{-3}$ Pa s of the buffer solution at 298 K) is given by Debye's expression^{2,23}

$$\tau_{\beta} = \frac{3V\eta}{k_B T} = \frac{4\pi a^3 \eta}{k_B T} \quad (8)$$

where k_B is the Boltzmann constant. RNase A can be pictured as an ellipsoid with an axial ratio of about 1.5. For this degree of anisotropy, more elaborate treatments²⁵ differ only marginally from those of eq 8, provided that a is interpreted as the radius of the equivalent sphere. Our results indicate that the hydrodynamic radius depends on protein concentration (Table 1). Extrapolation to infinite dilution yields $\tau_1 \approx 20$ ns, which by eq 8 yields $a = 1.94$ nm, in perfect agreement with the result obtained from ¹⁵N NMR¹⁶ and dynamic light scattering.⁴⁹ On the basis of correlations for the volume–molecular mass relationship of globular proteins,^{38,50} the intrinsic radius of RNase A is $a = 1.54$ nm.

Similar differences between intrinsic and hydrodynamic radii have been observed for other proteins and have played a key role in discussions of hydration properties deduced from dielectric relaxation data.² According to popular interpretations, such a difference indicates one or more layers of hydration water, bound to the protein at the time scale of protein tumbling, i.e., at least at nanoseconds. This is clearly at variance with the picture of a mobile hydration sphere and of short residence times.

As shown by Halle and Davidovic,³⁸ a more adequate model can resolve this paradox. A major ingredient is the use of the atomic level protein structure for estimating the radius of the real protein, as compared with an estimate for a sphere or ellipsoid. There are computer programs such as HYDROPRO,⁵¹ which, by bead-modeling methodologies, calculate the hydrodynamic radius from the coordinates of the nonhydrogen atoms of the protein structure together with a parameter, σ , which represents the average atomic volume. This brings the theoretical predictions already in fair agreement with experimental data.³⁸ The remaining discrepancies can be removed, when noting that the viscous friction is not adequately captured by a uniform viscosity of the medium. Rather, the local retardation of water at the protein surface suggests a spatially dependent viscosity. Halle and Davidovic³⁸ showed that such an approach rationalizes

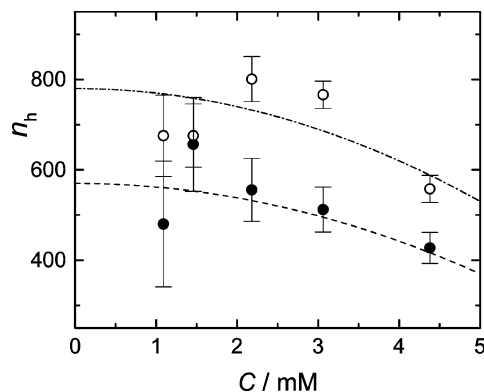


Figure 3. Hydration numbers derived from the amplitudes of γ -dispersion (filled symbols) and $\delta 3$ -dispersion (open symbols). Lines are drawn as a guide to the eye only.

the hydrodynamic radii of many proteins, including RNase A. While for details we refer to their paper, we re-emphasize that the observed hydrodynamic radius does by no means support the popular interpretation of hydrodynamic radii in terms of long-lived hydration.

Hydration Numbers. Many attempts were made to deduce from dielectric data values for hydration numbers, n_h , reflecting the number of water molecules affected by the protein. A common procedure is to derive n_h from the hydrodynamic radius. An alternative method calculates n_h from the amplitude S_γ of bulk water relaxation, which is extractable with high accuracy. S_γ decreases with increasing protein concentration, because water is diluted by the solute. By working out the dilution effect and comparing with experimental data, it is found that some further waters must have disappeared from the spectral regime of γ -dispersion, presumably due to retarded motions in the hydration sphere, which in turn enables the calculation of n_h by more or less sophisticated models.^{21,52}

In practice, Kaatz³ has constructed a master curve for the dilution effect based on data for simple solutes and nonionic polymers. At the protein concentrations considered here, this curve can be fitted to the linear equation $S_\gamma = 73.0 (1 - 0.989 \times 10^{-3} C \text{ (mM)})$. By comparison with experiment, it is then straightforward to extract n_h . Considering this simple approach, the results in Figure 3 are in surprisingly good agreement with 470 hydration waters, estimated from the solvent accessible surface area of RNase A deduced from the crystal structure.⁶ This agreement should, however, be regarded with caution. A rigorous treatment of the dilution effect has to consider the depolarizing electric fields in the dielectrically heterogeneous regions of the sample. Thereby, it is explicitly or implicitly assumed that the protein forms a “dielectric void” of low permittivity. MD simulations indicate a highly polar surface.^{9,10}

Another option is to estimate n_h from the amplitude $S_{\delta 3}$ of hydration water relaxation. In doing so, practically all methods assume the effective mean square dipole moment, μ_{eff}^2 , of water molecules in the hydration layer to be equal to the value in the bulk. Then, the ratio $S_{\delta 3}/S_\gamma$ is proportional to the ratio of the water contents in the two environments, which immediately yields n_h . The resulting hydration numbers (Figure 3) are higher than those calculated from bulk water relaxation. While one cannot go far beyond this simple model, we note that the squared effective dipole moment of water is given by²³

$$\mu_{\text{eff}}^2 = g_K \mu_o^2 \quad (9)$$

where $\mu_o = 1.84 \text{ D}$ is the dipole moment of the isolated

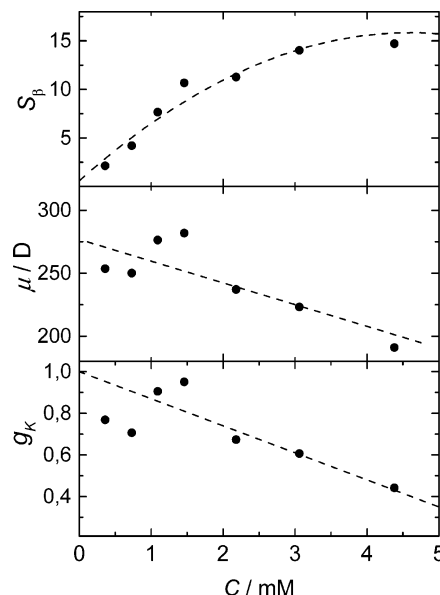


Figure 4. Amplitude (S_β) of the protein tumbling mode, effective dipole moments (μ_{eff}), and protein–protein Kirkwood factors (g_K) as a function of composition.

molecule. An increase of $g_{K,H}$ over the bulk value, as suggested earlier, thus causes an overestimate of n_h .

Dipole Moments of Proteins. The amplitude of the protein tumbling mode, S_β , provides the protein’s dipole moment, but such calculations have to rely on a dielectric model. We adopt here the Onsager–Oncley model, which relates the effective dipole moment of the protein in solution to the amplitude by²

$$\mu_{\text{eff}}^2 = \frac{2kT\epsilon_o S_\beta}{N_A C} \quad (10)$$

Slightly different expressions for other dielectric models² lead to dipole moments that typically differ by up to 10% from that extracted by eq 10.

Figure 4 shows a flattening of the S_β vs C curve, i.e., a decrease of μ_{eff}^2 with increasing protein concentration. Hitherto, such a concentration dependence remained unnoticed. Again, the effective dipole moment is related to that of the isolated protein via eq 9, and the observed concentration dependence of μ_{eff}^2 can only be found in a decrease of the Kirkwood factor g_K . Hitherto, all dipole moment determinations presumed that $g_K = 1$,² implying the absence of orientational correlations. The argument is that numerous solute–solvent forces act on a rotating protein over a wide range of directions, thus mimicking random protein–water dipolar correlations.^{2c} However, this argument does not account for protein–protein dipolar correlations at finite protein concentrations.

The determination of g_K requires the dipole moment of the protein in the absence of dipolar correlations. In real systems, μ_o depends on the net charge of the protein, which is dictated by the pH of the solution. Preliminary experiments in our laboratory indeed indicated a pH-dependent dipole moment of RNase A.⁵³ As noted by Antosiewicz,^{36b} many experimental dipole moment values for proteins are of little value, because the conditions controlling the net charge of the protein are not specified. For similar reasons, older estimates of dipole moments from increments for peptides, extensively discussed in textbooks,² are of little practical value. The only reasonable way to evaluate the Kirkwood factor in an accurate way is therefore to determine μ_o experimentally by extrapolation of the effective

dipole moment to zero concentration of the protein. By such a procedure, we find that $\mu_o = 280$ D. The uncertainty of the data at low concentrations may allow a steeper extrapolation, so that this value is a lower limit. Note that Antosiewicz^{36b} calculated from the protein structure of RNase A at the isoelectric point (pI = 9.3, coordinated metal ions included) $\mu_o = 350$ D.

The dependence of the dipole moment on buffer, pH and protein concentration renders comparison with literature data difficult. Two previous dielectric studies of RNase A have yielded $\mu_{\text{eff}} = 350$ D ($w_P = 0.02$, 10 mM NaCl, pH 2.7)¹⁸ and $\mu_{\text{eff}} = 100$ D ($w_P = 0.06$, probably free of buffer, pH not specified).¹⁹ Even when accounting for a strong dependence on the solution conditions, the latter value seems to be in error, possibly because of an insufficient sampling of the β -mode at low frequencies.

Figure 4 shows that g_K decreases with increasing protein concentration. Such a behavior cannot be attributed to changes in the hydration structure but must result from strong antiparallel dipolar correlations between protein molecules, obviously favored by their high dipole moments. This also rationalizes the increase of the hydrodynamic radius with increasing concentration (Table 1). It is known that RNase A does not form distinct aggregates such as dimers or multimers. The second osmotic virial coefficient indicates, however, protein–protein interactions, which sensitively depend on the pH and nature of the buffer.⁴⁶ Thus, the Kirkwood factor reflects mutual compensation of dipole moments due to nonspecific, electrostatic interactions, as often encountered in simple systems.²³ This pronounced sensitivity to dipolar orientational correlations opens interesting possibilities for studying electrostatic protein–protein interactions, for example, of relevance for diffusion-controlled rate processes.⁵⁴ Thus, before two proteins associate to form a complex, they have to find the proper relative orientation by rotational diffusion. Orientational constraints can therefore severely limit the rate of association.⁵⁴ Orientational correlations due to dipolar interactions between proteins may therefore lead to notable electrostatic steering of protein–protein associations, in addition to the effect of the direct Coulombic interactions between charged groups.

5. Conclusions

Dielectric spectroscopy is a valuable tool for studying the structure and dynamics of protein solutions. In the past, many studies have addressed the so-called δ -relaxation, but as rightly noted by Kaatze,³ interpretations are difficult, because diverse dynamical processes may drive dipole moment fluctuations. Moreover, dielectric relaxation observes fluctuations of the total dipole moment of the sample rather than of distinct molecular dipoles. This may cause dipolar cross-correlations to control some of the dielectric modes, which are not easily described by simple models for reorientational dynamics. This complexity requires the proper embedding of dielectric relaxation in the framework of other methods such as NMR techniques and MD simulations.

In this study, we have applied such a concerted approach to single out the information extractable from dielectric spectra. Thereby, it has become evident that some popular concepts used in data interpretation do not withstand this test. In fact, as emphasized by Finney,^{1b} in the past decade, there has been a change in paradigm with regard to hydration dynamics of proteins: For a long time, the picture of long-lived, rigid protein hydration has prevailed, and much of this picture has resulted from dielectric relaxation studies. It is now known that the

hydration layer is highly mobile, with regard to both molecular reorientation and translational hydration water–bulk water exchange. In dielectric relaxation work, these developments have been rather unnoticed.

In our opinion, the assignment suggested here forms the only option, which is consistent with the more recent results from other experiments and simulations. In particular, the consideration of collective contributions rationalizes the presence of modes that are not observed by other experimental techniques. The presence of such dipolar correlations is widely recognized in interpretations of static dielectric constants of simple systems, and an understanding of their role for dynamic processes is just beginning to evolve. For biomolecular systems, the role of collective modes has recently been repeatedly emphasized,^{11,12,27} although some of the suggested models for cross-correlations²⁷ use a model of long-lived hydration and thus do not withstand critical examination. The present study suggests that such cross-correlations do not only modify the relaxation amplitudes via the static Kirkwood factor but can even give rise to distinct modes in the spectrum. From the perspective of applications, a well-established assignment of the various processes opens a sound basis for addressing more specific problems, for example, associated with protein–solvent and protein–protein interactions.

Acknowledgment. The financial support of the Deutsche Forschungsgemeinschaft within the research network FOR 436 at the universities of Dortmund and Bochum (“Polymorphism, dynamics and function of water at molecular interfaces”) is gratefully acknowledged. Profs. O. Steinhauser (Vienna), B. Halle (Lund), and R. Winter (Dortmund) are thanked for extensive and very fruitful discussions.

References and Notes

- (1) (a) Gregory, R. B., Ed. *Protein–Solvent Interactions*; Marcel Dekker: New York, 1995. (b) Finney, F., Ed.; *Faraday Discuss. Chem. Soc.* **1996**, 103.
- (2) (a) Grant, E. H.; Sheppard, R. J.; South, P. G. *Dielectric Behaviour of Biological Molecules in Solutions*; Clarendon: Oxford, 1978. (b) Takashima, S. *Electrical Properties of Biopolymers and Membranes*; Adam Hilger: Bristol, 1989. (c) Pethig, R. *Annu. Rev. Phys. Chem.* **1992**, 43, 177.
- (3) Kaatze, U. *Phys. Med. Biol.* **1990**, 35, 1663.
- (4) See, for example, Svergun, D. I.; Richard, S.; Koch, M. H. J.; Sayers, Z.; Kuprin, S.; Zaccai, G. *Proc. Natl. Acad. Sci. U.S.A.* **1998**, 95, 2267.
- (5) (a) Denisov, V. P.; Halle, B. In ref 2, p 227. (b) Halle, B. In *Hydration Processes in Biology*; Bellissent-Funel, M. C., Ed.; IOS: Amsterdam, 1998; pp 233–249.
- (6) Denisov, V. P.; Halle, B. *Biochemistry* **1998**, 37, 9595.
- (7) Modig, K.; Liepinsh, E.; Otting, G.; Halle, B. *J. Am. Chem. Soc.* **2004**, 126, 102.
- (8) (a) Abseher, R.; Schreiber, H.; Steinhauser, O. *Proteins* **1996**, 25, 266. (b) Marchi, M.; Stapone, F.; Ceccarelli, M. *J. Am. Chem. Soc.* **2002**, 124, 6787. (c) Bizzarri, A. R.; Cannistraro, S. *J. Phys. Chem. B* **2002**, 106, 6617.
- (9) (a) Simonson, T. *Rep. Prog. Phys.* **2003**, 66, 737. (b) Simonson, T.; Perahia, D. *Faraday Discuss. Chem. Soc.* **1996**, 103, 71 and references cited therein.
- (10) Smith, P. E.; Brunne, R. M.; Mark, A. E.; van Gunsteren, W. F. *J. Phys. Chem.* **1993**, 97, 2009.
- (11) Löffler, G.; Schreiber, H.; Steinhauser, O. *J. Mol. Biol.* **1997**, 270, 520.
- (12) Boresch, S.; Höchtel, P.; Steinhauser, O. *J. Phys. Chem. B* **2000**, 104, 8743.
- (13) Raines, R. T. *Chem. Rev.* **1998**, 98, 1045.
- (14) Wlodawer, A.; Svensson, L. A.; Sjölin, L.; Gilliland, G. L. *Biochemistry* **1988**, 27, 2705. Protein Data Bank (PDB) entry code 7rsa.
- (15) Merlino, A.; Vitagliano, L.; Ceruso, M. A.; Di Nola, A.; Mazzarella, L. *Biopolymers* **2002**, 65, 274.
- (16) Cole, R.; Loria, J. P. *Biochemistry* **2002**, 41, 6072.
- (17) Rasmussen, B. F.; Stock, A. M.; Ringe, D.; Petsko, G. A. *Nature* **1992**, 357, 423.

- (18) Feldman, Yu. D.; Fedotov, V. D. *Chem. Phys. Lett.* **1988**, *143*, 309.
- (19) Abou-Aiad, T.; Becker, U.; Biedenkamp, R.; Brengelmann, R.; Elsebrock, R.; Hinz, H.-J.; Stockhausen, M. *Ber. Bunsen-Ges. Phys. Chem.* **1997**, *101*, 1921.
- (20) Sasisanker, P.; Oleinikova, A.; Weingärtner, H.; Ravindra, P.; Winter, R. *Phys. Chem. Chem. Phys.* **2004**, *6*, 1899. This paper shows the DSC trace of our batch of RNase A at the pH used by us. Denaturation sets in at 55 °C.
- (21) del Rosario, E. J.; Hammes, G. G. *Biochemistry* **1968**, *8*, 1884.
- (22) Göttmann, O.; Kaatze, U.; Petong, P. *Meas. Sci. Technol.* **1996**, *7*, 525.
- (23) Böttcher, C. J. F.; Bordevijs, P. *Theory of Dielectric Polarisation*; Elsevier: Amsterdam, 1973; Vol. 1; 1978; Vol. 2.
- (24) Kaatze, U. *J. Chem. Eng. Data* **1993**, *38*, 1.
- (25) Perrin, F. *J. Phys. Radium* **1936**, *7*, 1.
- (26) See, for example, de Boer, C. *A Practical Guide to Splines*; Springer: New York, 1978.
- (27) (a) Nandi, N.; Bagchi, B. *J. Phys. Chem. A* **1997**, *101*, 10954. (b) Nandi, N.; Bagchi, B. *J. Phys. Chem. A* **1998**, *102*, 8217. (c) Nandi, N.; Bhattacharyya, K.; Bagchi, B. *Chem. Rev.* **2000**, *100*, 2013.
- (28) Ladanyi, B. M.; Skaf, M. S. *J. Chem. Phys.* **1996**, *100*, 1368.
- (29) Kaatze, U. *J. Solution Chem.* **1997**, *26*, 11 and references cited therein.
- (30) Weingärtner, H.; Knocks, A.; Boresch, S.; Höcht, P.; Steinhäuser, O. *J. Chem. Phys.* **2001**, *115*, 1463.
- (31) Knocks, A.; Weingärtner, H. *J. Phys. Chem. B* **2001**, *105*, 3635.
- (32) (a) Weingärtner, H.; Volmari, A. *J. Mol. Liquids* **2002**, *98/99*, 293 and references therein. (b) Weingärtner, H.; Nadolny, H.; Oleinikova, A.; Ludwig, R. *J. Chem. Phys.* In press.
- (33) Madden, P.; Kivelson, D. *Adv. Chem. Phys.* **1984**, *56*, 467.
- (34) See, for example, Saiz, L.; Guàrdia, E.; Padró, J. A. *J. Chem. Phys.* **2000**, *113*, 2814.
- (35) (a) Takashima, S.; Asami, K. *Biopolymers* **1993**, *33*, 59. (b) Antosiewicz, J. *Biophys. J.* **1995**, *69*, 1344. For species with net charge, the calculated dipole moment depends on the reference frame.²³
- (36) Korzhnev, D. M.; Billeter, M.; Arseniev, A. S.; Orekhov, V. Y. *Prog. Nucl. Magn. Reson. Spectrosc.* **2001**, *38*, 197.
- (37) Gardner, K. H.; Kay, L. E. *Biol. Magn. Reson.* **1998**, *16*, 27–74.
- (38) Halle, B.; Davidovic, M. *Proc. Natl. Acad. Sci. U.S.A.* **2003**, *100*, 12135.
- (39) Kirkwood, J. G. *J. Chem. Phys.* **1936**, *4*, 592.
- (40) Merzel, F.; Smith, J. C. *Proc. Natl. Acad. Sci. U.S.A.* **2002**, *99*, 5378.
- (41) Giese, K. *Ber. Bunsen-Ges. Phys. Chem.* **1972**, *76*, 495.
- (42) See, for example, Otting, G.; Liepinsh, E.; Wüthrich, K. *Science* **1991**, *254*, 974.
- (43) Makarov, V. A.; Andrews, K. B.; Smith, P. E.; Pettitt, B. M. *Biophys. J.* **2000**, *79*, 2965.
- (44) Halle, B. *J. Chem. Phys.* **2003**, *119*, 12372.
- (45) Malamud, D.; Drysdale, J. W. *Anal. Biochem.* **1978**, *86*, 620.
- (46) Tessier, P.; Johnson, H. R.; Pazhianur, R.; Berger, B. W.; Prentice, J. L.; Bahnson, B. J.; Sandler, S. I.; Lehnhoff, A. M. *Proteins* **2003**, *50*, 303.
- (47) Barr, Ch.; Buchner, R.; Kunz, W. *J. Phys. Chem. B* **2001**, *105*, 2914.
- (48) Grosse, C. *J. Phys. Chem.* **1988**, *92*, 3905.
- (49) Noeppert, A.; Gast, K.; Müller-Frohne, M.; Zirwer, D.; Damaschun, G. *FEBS Lett.* **1996**, *380*, 179.
- (50) Chalikian, T. V.; Breslauer, K. J. *Biopolymers* **1996**, *39*, 619.
- (51) Garcia de la Torre, J.; Huertas, M. L.; Carrasco, B. *Biophys. J.* **2000**, *78*, 719.
- (52) (a) Wei, Y. Z.; Khumbarkhane, A. C.; Sadeghi, M.; Sage, J. T.; Tian, W. D.; Champion, P. M.; Shridhar, S.; McDonald, M. J. *J. Phys. Chem.* **1994**, *98*, 6644. (b) Yokoyama, K.; Kamei, T.; Miami, H.; Suzuki, M. *J. Phys. Chem. B* **2001**, *105*, 12622.
- (53) Sasisanker, P.; Oleinikova, A.; Weingärtner, H. To be published.
- (54) (a) Vijayakumar, M.; Wong, K.-Y.; Schreiber, G.; Fersht, A. R.; Szabo, A.; Zhou, H.-X. *J. Mol. Biol.* **1998**, *278*, 1015. (b) Schreiber, G.; Fersht, A. R. *Nat. Struct. Biol.* **1996**, *3*, 427.